applied sciences

MDPI

Article

Hybridizing Lithography-Based Ceramic Additive Manufacturing with Two-Photon-Polymerization

Johanna Christiane Sänger [1,2,*], Martin Schwentenwein [3], Raúl Bermejo [1] and Jens Günster [2,4,*]

[1] Department of Materials Science, Montanuniversität Leoben, Franz Josef Strasse 18, 8700 Leoben, Austria
[2] Federal Institute for Materials Research and Testing (BAM), Unter den Eichen 87, 12205 Berlin, Germany
[3] Lithoz GmbH, Mollardgasse 85a/2/64-69, 1060 Vienna, Austria
[4] Institute of Non-Metallic Materials, Clausthal University of Technology, Zehntnerstraße 2A, 38678 Clausthal-Zellerfeld, Germany
* Correspondence: johanna.saenger@unileoben.ac.at (J.C.S.); jens.guenster@bam.de (J.G.); Tel.: +43-(0)-3842-402-4125 (J.C.S.); +49-(0)-30-8104-1540 (J.G.)

Abstract: Stereolithography processes such as lithography-based ceramic manufacturing (LCM) are technologies that can produce centimeter-sized structures in a reasonable time frame. However, for some parts specifications, they lack resolution. Two-photon-polymerization (2PP) ensures the highest geometric accuracy in additive manufacturing so far. Nevertheless, building up parts in sizes as large as a few millimeters or even centimeters is a time-consuming process, which makes the production of 2PP printed parts very costly. Regarding feedstock specification, the requirements for 2PP are different to those for LCM, and generally, feedstocks are designed to meet requirements for only one of these manufacturing technologies. In an attempt to fabricate highly precise ceramic components of a rather large size, it is necessary to develop a feedstock that suits both light-based technologies, taking advantage of LCM's higher productivity and 2PP's accuracy. Hybridization should bring the desired precision to the region of interest on reasonably large parts without escalating printing time and costs. In this study, specimens gained from a transparent feedstock with yttria stabilized zirconia (YSZ) particles of 5 nm at 70 wt% were presented. The resin was originally designed to suit 2PP, while being also printable with LCM. This work demonstrates how hybrid parts can be sintered into full YSZ ceramics.

Keywords: ceramic; additive manufacturing; transparent feedstock; hybridization; powder processing; yttria stabilized zirconia

check for updates

Citation: Sänger, J.C.; Schwentenwein, M.; Bermejo, R.; Günster, J. Hybridizing Lithography-Based Ceramic Additive Manufacturing with Two-Photon-Polymerization. *Appl. Sci.* **2023**, *13*, 3974. https://doi.org/10.3390/app13063974

Academic Editor: Soshu Kirihara

Received: 20 February 2023
Revised: 16 March 2023
Accepted: 17 March 2023
Published: 21 March 2023

Copyright: © 2023 by the authors. Licensee MDPI, Basel, Switzerland. This article is an open access article distributed under the terms and conditions of the Creative Commons Attribution (CC BY) license (https://creativecommons.org/licenses/by/4.0/).

1. Introduction

The additive manufacturing (AM) of ceramics in the micrometer scale opens new applications, associated with their inherent unique properties such as thermally stability, chemical inertness, abrasion resistance, biocompatibility and various functional properties [1]. Due to the large surface volume ratio of microstructures, corrosion and chemical resistance play an important role. Conventional ceramic processing of very small structures is expensive and often limited by geometry (e.g., wall thickness). In such cases, AM-technologies can help to create ceramic structures in unmatched shapes. One of those technologies is two-photon polymerization (2PP), which enables the highest accuracy of all AM-technologies so far. Feature sizes below 100 nm have been reported [2]. This accuracy has so far been applicable to a few types of resins, such as homogeneous polymers, nano-composites, bio-polymers [3] and polymer derived ceramics (PDCs) [4]. All these systems meet one major requirement for 2PP, which is transparency. This concept has been successfully transferred to a ceramic slurry of 70 wt% yttria stabilized zirconia (YSZ) nano-particles [5]. The zirconia slurry can provide high transmittance in the relevant wavelength range of around 800 nm together with a high-solid loading, thus enabling the manufacturing of technical ceramics utilizing the 2PP process.

Even though the opportunities opened by this new feedstock are thrilling, the achievement comes with a major drawback. Printing millimeter- or even centimeter-sized features with 2PP-accuracy takes a tremendously long processing time, making this approach excessively expensive for the manufacture of macroscopic parts. In this regard, there are technologies in development to speed up 2PP-printing, e.g., using parallel beams or increasing the scanning speed. However, they may not reach the printing speed of larger vat-photopolymerization (VPP) techniques, such as lithography-based ceramic manufacturing (LCM). Combining the accuracy of 2PP with the printing speed of LCM appears, in this context, to be very appealing [6]. Chemistry-wise, the process is the same, as only different photo-initiators are needed. The same principle has been already tested with PDCs [7], which are suitable for both 2PP and LCM.

In order to apply the 2PP process to ceramic slurries, a certain level of transparency is required. Hybridizing 2PP with stereolithography, in particular LCM, is not naturally given, as feedstocks for LCM are generally not transparent for the light used to crosslink the photoactive slurry. The light might penetrate too deep into the slurry and definition of the part in z-direction may be lost. On the other hand, for crosslinking more massive structures in one UV-illumination event with a conventional UV lamp, e.g., for the generation of flat substrates to support 2PP structures of the same material [5], an even higher transmissivity is required.

The present study takes the advantage of the fact that the transparent 2PP-resins are printable with stereolithography technologies. The first results in hybridizing these two technologies are presented on a zirconia material, and it is demonstrated that the YSZ feedstock can be used for 2PP printing, crosslinking substrates with a UV lamp and the LCM process. Moreover, the specimens fabricated are generated from the same slurry-composition, and successively printed with 2PP onto LCM-manufactured parts and UV-cured substrates. It is not only possible to print structures with 2PP in high resolution onto macroscopic substrates, but also the UV-cured, or LCM-manufactured structures can be sintered together with 2PP features, resulting in a uniform shrinkage with low distortion in the filigree 2PP structures.

2. Materials and Methods

2.1. Material Preparation and Characterization

The feedstock for both processes was a photocurable poly-(ethylenglykol) diacrylate (PEG-DA) resin (average Mn = 250, Sigma-Aldrich, St. Louis, MO, USA) with 70 wt% of yttria stabilized zirconia nanoparticles (nanoBinder, CeraNovis GmbH, Saarbrücken, Germany). For 2PP processing and UV curing the photoinitiators 2,5-bis-[4-[N,N-bis-[2-(acetyloxy)ethyl]phenyl]-methylene]-(2E,5E)-cyclopentanone (BAE, Genosynth) and 2,2-dimethoxy-2-phenylacetophenon (DMPA, Sigma-Aldrich) were used, respectively.

UV–vis transmission measurements inside cleavable quartz cuvettes (Hellma Analytics, Müllheim, Germany) with a thickness of 0.1, 0.5 and 10 mm were performed using a BLACKComet C-50 spectrometer (StellarNet Inc., Keystone, FL, USA) with an SL5 deuterium halogen light source.

LCM was performed using a 3D-printing system based on a digital light processing (DLP) setup with a bottom-up printing approach (CeraFab S65, Lithoz GmbH, Vienna, Austria), which uses blue LEDs with a wavelength of 455 nm [8,9]. The nominal lateral resolution of this printer is 40 µm. For the printing experiments with the nano-sized YSZ slurry, green parts were printed with 25 µm layers. After printing, the resulting green parts were cleaned using pressurized air before these parts were used for the 2PP experiments.

2.2. 2PP Printing Setup

3D printing was performed using a two-photon polymerization instrument (Nanofactory, Femtika, Ltd., Vilnius, Lithuania) [10], employing a femtosecond laser light source (C-Fiber 780 High Power, Menlo Systems GmbH, Planegg, Germany) operating at 100 fs pulse duration, 100 MHz repetition rate, and 780 nm wavelength. The laser

was passed through a 60 × 1.4/20 × 0.45 numerical aperture air objective (Nikon Corporation, Tokyo, Japan). The positioning system combined linear stages ANT130XY-160 (Aerotech Inc., Pittsburgh, PA, USA) for the x-y plane, ANT130LZS-060 (Aerotech Inc.) for the Z-direction, and galvo-scanners (AGV-10HPO (Aerotech Inc.) for image projection. Programming tasks and controlling the process were done by 3DPoli software (Femtika Ltd.).

2.3. 2PP Printing Process

Printing geometries and their STL-files were obtained from an open-source platform. Simple geometries, such as cubes, were modeled manually. Special geometries, such as the SchwarzP tripleperiodic minimal surface structure [11], were produced using in-house developed software [12] based on an open-source software for the design of tissue engineering scaffolds [13]. Haptic objects were scanned with a GOM-scanner (Carl Zeiss AG, Jena, Germany). Transformation of the STL format into machine-readable G-Code was realized by the open-source software Ultimaker Cura (4.8.0) [14]. The CAD models were translated into G-Codes for each single structure.

In the present study, two types of macroscopic structures were serving as substrates for the 2PP process: (i) structures simply generated by UV curing of a thin layer of the resin and (ii) structures manufactured by the LCM process. UV cured and LCM manufactured substrates were taped onto a glass slide and several layers of adhesive tape were used for providing room for the 2PP-resin and 2PP printing (Figure 1). A thin cover glass was used as a lid for the printing envelope. All structures were printed with a speed of 10,000 µm s^{-1} and a power of 8 mW.

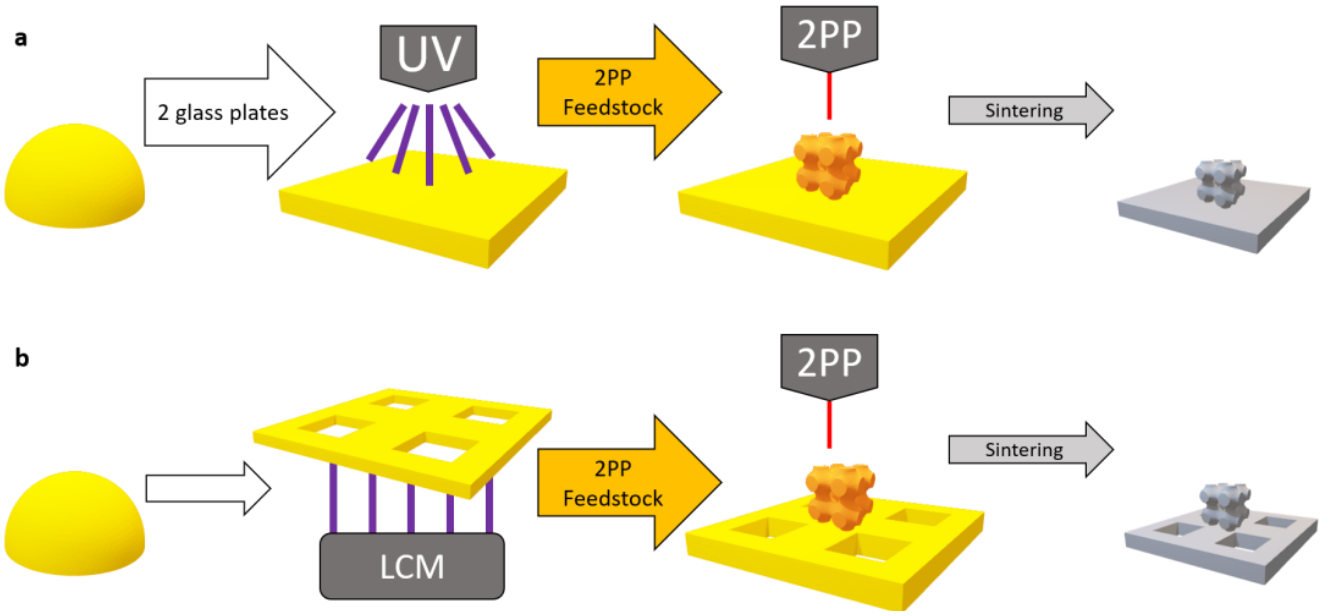

Figure 1. Process chain to generate hybrid specimens: (**a**) starting with a substrate generated with UV-light in between two glass plates; and (**b**) starting with a UV-curable substrate structured with LCM. In both routes the 2PP-feedstock is added afterwards as a single droplet followed by the 2PP-printing.

Printed structures were washed using ethanol (absolute water free min. = 99.5%, Sigma-Aldrich) to remove uncured material. After washing, the structures were dried via critical point drying (EM CPD300, Leica, Wetzlar, Germany).

Thermal debinding and sintering was performed in a high temperature oven (HTF 17/10, Carbolite Gero GmbH, Neuhausen, Germany) with a controller (Eurotherm 2416, Eurotherm Germany GmbH, Limburg an der Lahn, Germany) with the following temperature schedule: 0 → 150 °C (1 K min^{-1}) → 250 °C (0.1 K min^{-1}) → 265 (1 K min^{-1}) → 300 °C (0.1 K min^{-1}) → 350 °C (1 K min^{-1}) → 400 °C (0.1 K min^{-1}) → 800°C (1 K min^{-1}, dwell 2 h) → 0 °C (5 K min^{-1}). The Eurotherm-controller allows a programming of the tem-

perature ramps in a wide range. Absolute precision of the furnace at the sample position is approximately in the range of ±10 °C.

2.4. Microscopy Analysis and Mechanical Characterization

For the structural characterization of printed samples, a light microscope (VHX 7000, Keyence, Osaka, Japan) and a scanning electron microscope (EVO MA10, Carl Zeiss GmbH, Jena, Germany) were employed.

A cross-sectional cut was performed using a focused ion beam (FIB)/scanning electron microscope (SEM) system (Quanta 3D FEG, FEI Company, Hillsboro, OR, USA) equipped with a gallium source. After localizing the region of interest, a protective and smoothing platinum layer was deposited on the surface using an in situ chemical vapor deposition system. A surrounding volume material was excavated, and a fiducial structure was generated for beam alignment. Subsequently, the volume was cut using an acceleration voltage of 30 kV and a current of 30 nA, successively, decreasing to 7 nA and finally 1 nA. After cutting, an SEM image was taken.

3. Results and Discussion

3.1. Transparent YSZ Resin

Figure 2 shows the transmission through a 45 wt% YSZ slurry as a function of the wavelength of the incident light and as a function of the penetration depth, that is, the sample thickness. Cuvettes of different thickness were filled with the slurry and introduced into the photo spectrometer. Additionally, to the YSZ slurries, the YSZ PEG-DA resin with 70 wt% solid loading was measured. With increasing sample thickness, the intensity was drastically reduced. The intensity as a function of the sample thickness should show an exponential behavior of the type: $I_{(x)} = I_0 \exp(-\alpha x)$, following the Lambert–Beer law of absorption, with I_0 being the intensity of the incident light, $I_{(x)}$ the intensity of the light after passing a given length x through the material, and α the absorption or scattering coefficient. For the relevant wavelengths, around 400 nm for the UV lamp and LCM and around 800 nm for 2PP, transmission values are acceptable at 0.1 mm and 0.5 mm sample thickness.

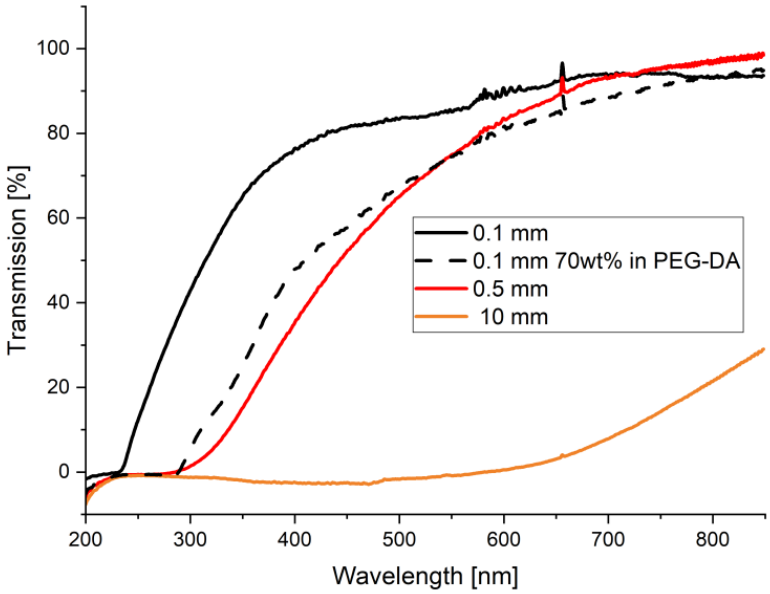

Figure 2. Transmission through a 45 wt% YZT slurry as a function of the wavelength of the incident light and as a function of the penetration depth, that is, the sample thickness. Also shown, the YSZ PEG-DA resin with 70 wt% solid loading.

3.2. Hybrid Printing

2PP structures were printed on a UV-cured substrate, with the substrate and the printed structures being from the same material. To create the UV-cured substrate, just the

2PP-photoinitiator (BEA) was exchanged by DMPA, which is sensitive to UV-light. For more details see also reference [5]. The procedure to combine UV-substrates with 2PP was as follows (Figure 3a): First, a drop of UV-curable resin was placed in between two glass plates and illuminated (crosslinked) with UV light from a conventional UV lamp. Exposure times are typically 10–30 s. Then, the 2PP curable resin was placed on top of the solid substrate and is crosslinked with the 2PP-Printer. Both the substrate and 2PP-structure were thermally treated to remove the organic binder and to sinter the ceramic particles. Figure 3a shows such a substrate before sintering and Figure 3b after sintering.

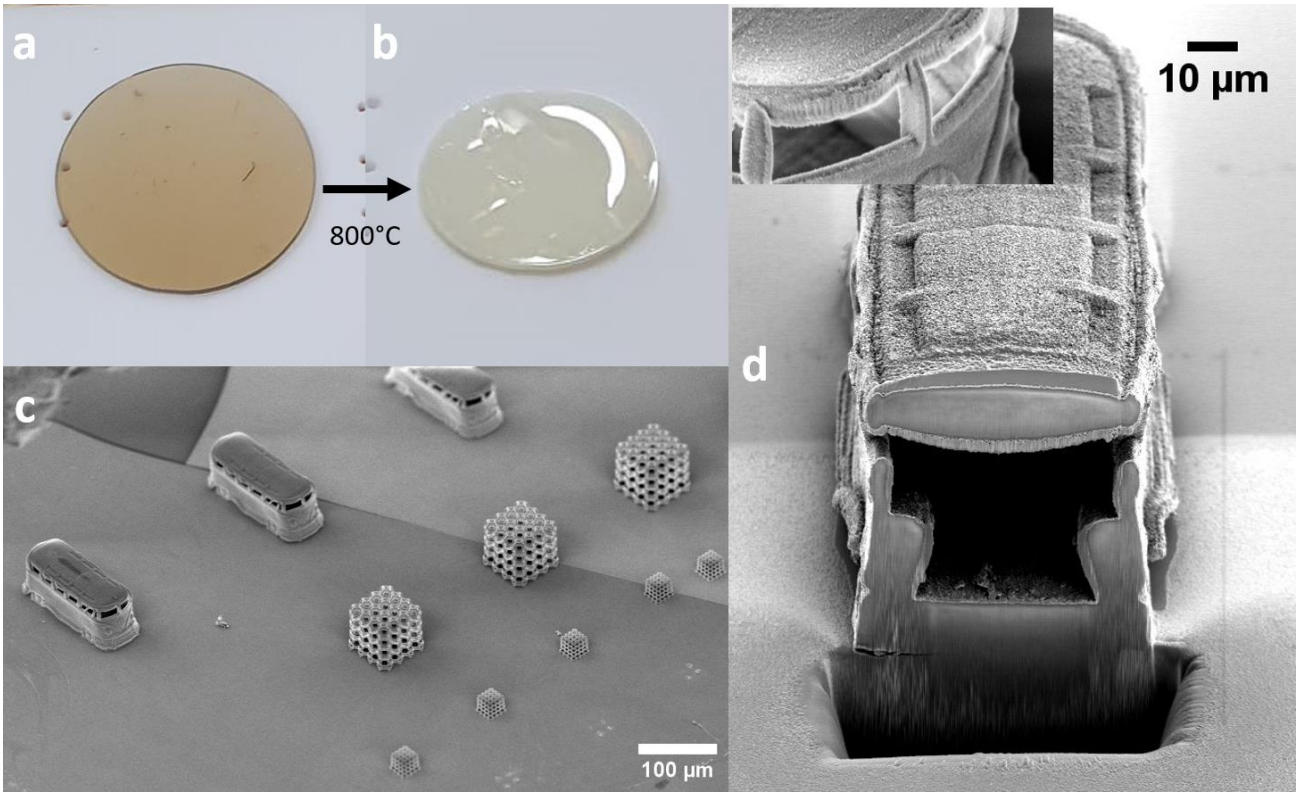

Figure 3. UV-cured substrate from 70 wt% yttria stabilized zirconia resin: (**a**) before; and (**b**) after sintering at 800 °C; (**c**) overview of 2PP-printed parts from the same resin on one substrate after sintering to 800 °C; and (**d**) FIB-cut of one bus plus detailed front view.

The area of the substrate generated according to the routes described in Figure 1a,b is relatively large compared to the size of 2PP-printed features, which allows for the printing of a variety of structures on one substrate. Figure 3c gives an overview of different 2PP-printed parts (i.e., micro-buses and lattice cube structures) on the UV-cured and sintered substrate. There is a row of micro-busses and two other rows of lattice cubes printed in different sizes. A FIB-cut (Figure 3d) through one bus shows the precision of the 2PP-printing process. The bus is hollow, its roof only sustained by the window pillars. The roof sagged slightly, because it is widely overhanging, but nevertheless the freestanding structure is strong enough to self-support. This example is not chosen to show the maximum accuracy of the process, which can be appreciated in reference [5], but it is a reminder of the freedom in design by employing AM technologies.

In a further printing job, the procedure is changed slightly as depicted in Figure 1b to combine 2PP with LCM. The UV curable resin is printed with an LCM machine to generate a structured substrate. Compared to the UV cure substrate procedure in Figure 1a, an additional washing step is required here to remove uncured resin from the printed LCM structure. Afterwards, the 2PP curable resin is added on top of it or in voids and

2PP printing can take place. The LCM- printed substrates with added 2PP-structures are sintered together.

One example is an LCM-printed clock hand, shown in Figure 4a, taped onto an objective slide, with tapes to generate space for the 2PP printing and with a small cover glass. This hybrid structure was sintered (Figure 4b). The arrows in Figure 4a indicate printed gearwheels on top of the clock-hand (Figure 4c). A comparison between non-sintered and sintered state shows a linear shrinkage of ~38%. Only one gearwheel was left after washing, which indicates a rather loose connection between the LCM print and 2PP sample. It is important to check the washing conditions after LCM printing, which might passivate the surface and therefore hinder a good connection to the 2PP print.

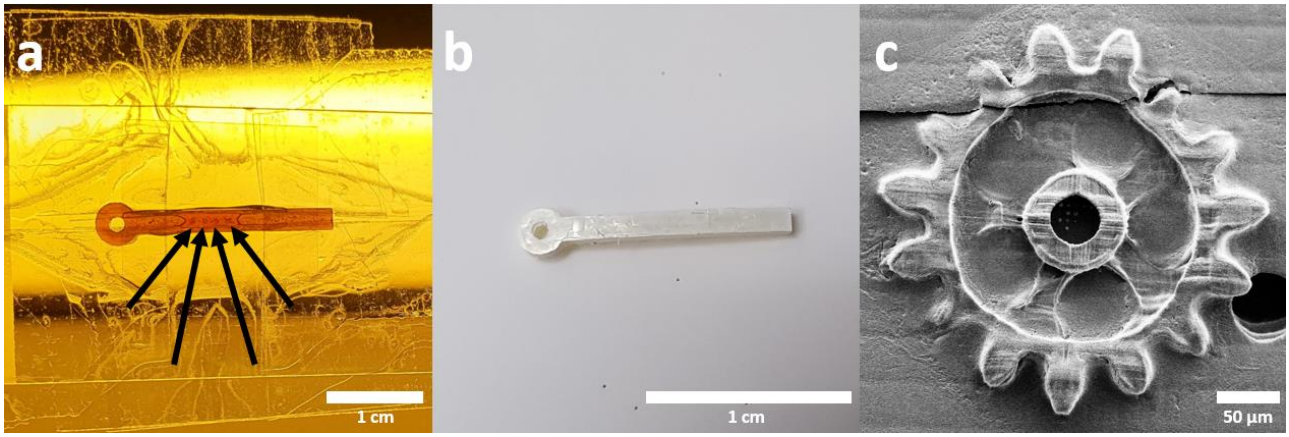

Figure 4. LCM printed clock-hand in: (**a**) non-sintered; and (**b**) sintered state with gearwheels on top of it, (**c**) SEM image of 2PP structure on top of the clock-hand.

The SEM-images also reveal a distortion of the gearwheel (Figure 4c). The smaller structure follows the inhomogeneous shrinkage of the supporting substrate, in this case the clock hand. The 2PP structure was printed with an air-objective, which provided a wider field of view (FOV). Single lines are visible in Figure 4c indicating too little overlap between the individual lines, which results in under-curing and also destabilizes the structures. Based on these first results, the best printing parameters are yet to be found.

Another challenge is to print inside voids or to print on top of open channels in the supporting substrate. This scenario is especially attractive as small nozzles, e.g., for fuel injection, could be structured on a micron scale to optimize fuel diffusion. To prove this concept, an LCM-printed plate with holes in it was employed as substrate. The 2PP resin was placed on top of it and was allowed to sink into the holes. A rather large SchwarzP-structure with 10 × 10 × 4 units was also printed bridging a void (Figure 5a). In Figure 5a it is already noticeable that the 2PP scaffold is cracked in the green state before sintering, which means that such filigree structures probably require special care during washing and drying. Nevertheless, the specimens were sintered successfully (Figure 5b–e) showing the same linear shrinkage of ~38% as the clock-hand in Figure 4. The LCM parts shrank with little distortion, as can be appreciated in Figure 5d. The SchwarzP structure did not develop any further distortion during sintering, which means that the debinding and sintering steps are not the most critical for 2PP-structures. The 2PP structure nicely covers the void, but probably the part above the surface induces stress during all post-processing steps. A detailed view of a single SchwarzP unit (Figure 5f) visualizes the single lines and layers, meaning that under-curing is an additional problem within this structure. This weakens the connection between the part on top and inside the void. Parts of features inside the void are visible in Figure 5c (white indicator). Apparently, the void is not filled completely within the XY-plane. Chunks of the SchwarzP structure might be lost during the printing process as the void is missing a support for the start of the print.

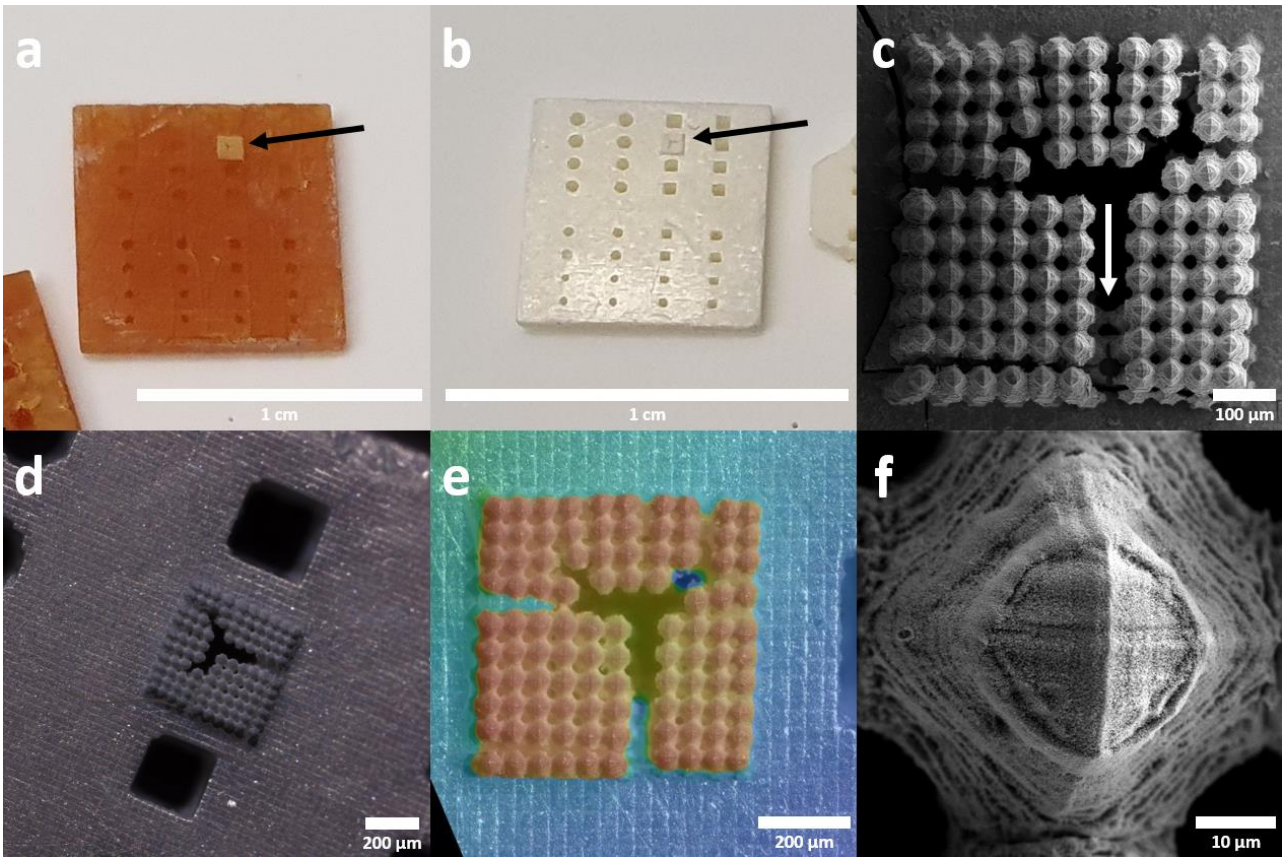

Figure 5. LCM printed plate with holes, (**a**) non-sintered, (**b**) sintered with 10 × 10 × 4 SchwarzP structure on top of it bridging a void, (**c**,**f**) sintered, SEM images, (**d**) sintered, light microscopy image, (**e**) sintered topological view.

From the results showed in this work, we deduce that both hybrid printing of LCM and 2PP structures and 2PP structures on UV cured substrates and their debinding and sintering to ceramic parts is feasible. Washing and drying after the 2PP process is critical to the 2PP structures due to capillary forces. Except of a relatively high linear shrinkage of ~38% during sintering, no significant distortion of the parts was noticeable. With the 2PP well connected to the LCM printed or UV cured substrate, sinter shrinkage was uniform and does not impose any additional deformation of the 2PP structures.

4. Conclusions

This study demonstrates the combination of lithography-based ceramic manufacturing LCM and two-photon-polymerization 2PP techniques, employing a transparent ceramic resin serving as feedstock. The hybridization of the two light-based additive manufacturing processes results in YSZ structures with local 2PP-resolution within parts of up to the centimeter size range. A connection between the two structures requires perfectly finished surfaces of the LCM parts. Topological effects, that is, rough surface and too harsh washing of the LCM structure, mismatch in particle fraction and polymer composition, too high viscosity or aging of the resin in general may result in a poor connectivity between LCM and 2PP structures (see Table 1). Choosing a milder washing procedure, or even omitting it eventually, should improve the connection. Washing after 2PP printing seems to be the most critical step in the generation of hybridized parts, as it imposes stresses by capillary forces onto the smallest structures. In addition, the printing strategy needs careful planning as well. For example, to fill voids the void should not be too deep, and the 2PP resin must cover it completely. On the other hand, as soon as a solid connection is established, the

features stay relatively unaffected by debinding and sintering, which appears promising for future applications.

Table 1. Summary of critical points for the success of Hybrid 2PP-LCM process.

Critical Point for Hybrid Process	Influence
Particle weight fraction	Same particle weight fraction in 2PP and LCM feedstocks ensures same shrinkage during sintering
Polymer composition	Same polymer composition in 2PP and LCM feedstocks ensures homogeneous degassing during debinding
Resin Viscosity	The 2PP resin viscosity shouldn't exceed a certain value that it can penetrate pores in LCM printed substrate
Washing and Drying of UV/LCM-part	Washing and Drying needs to be optimized to prevent passivation and roughening of the surface as well as cracking of the substrate

Author Contributions: Conceptualization, J.C.S. and J.G.; methodology, J.C.S. validation, J.G. and J.C.S.; writing—original draft preparation, J.C.S.; writing—review and editing, M.S., R.B. and J.G. All authors have read and agreed to the published version of the manuscript.

Funding: This research received no external funding.

Institutional Review Board Statement: Not applicable.

Informed Consent Statement: Not applicable.

Data Availability Statement: No new data were created or analyzed in this study. Data sharing is not applicable to this article.

Acknowledgments: The authors thank Frank Meyer, CEO CeraNovis GmbH, for the generous material support and Anna Lebhard for printing the support structures at Lithoz GmbH. Parts of this work was performed at the electron microscopy center at BAM, with special thanks to René Hesse at division 5.1. Raúl Bermejo acknowledges the European Research Council (ERC) excellent science grant "CERATEXT" through Horizon 2020 program under contract 817615.

Conflicts of Interest: The authors declare no conflict of interest.

References

1. Zocca, A.; Colombo, P.; Gomes, C.M.; Günster, J. Additive Manufacturing of Ceramics: Issues, Potentialities, and Opportunities. *J. Am. Ceram. Soc.* **2015**, *98*, 1983–2001. [CrossRef]
2. Faraji Rad, Z.; Prewett, P.D.; Davies, G.J. High-resolution two-photon polymerization: The most versatile technique for the fabrication of microneedle arrays. *Microsyst. Nanoeng.* **2021**, *7*, 71. [CrossRef] [PubMed]
3. Carlotti, M.; Mattoli, V. Functional Materials for Two-Photon Polymerization in Microfabrication. *Small* **2019**, *15*, 1902687. [CrossRef] [PubMed]
4. Bauer, J.; Crook, C.; Izard, A.G.; Eckel, Z.C.; Ruvalcaba, N.; Schaedler, T.A.; Valdevit, L. Additive manufacturing of ductile, ultrastrong polymer-derived nanoceramics. *Matter* **2019**, *1*, 1547–1556. [CrossRef]
5. Sänger, J.C.; Pauw, B.R.; Riechers, B.; Zocca, A.; Rosalie, J.; Maaß, R.; Sturm, H.; Günster, J. Entering a New Dimension in Powder Processing for Advanced Ceramics Shaping. *Adv. Mater.* **2022**, *35*, 2208653. [CrossRef] [PubMed]
6. Schwentenwein, M.; Schneider, P.; Homa, J. Lithography-based ceramic manufacturing: A novel technique for additive manufacturing of high-performance ceramics. In *Advances in Science and Technology*; Trans Tech Publications Ltd.: Stafa-Zurich, Switzerland, 2014; Volume 88, pp. 60–64.
7. Schmidt, J.; Brigo, L.; Gandin, A.; Schwentenwein, M.; Colombo, P.; Brusatin, G. Multiscale ceramic components from preceramic polymers by hybridization of vat polymerization-based technologies. *Addit. Manuf.* **2019**, *30*, 100913. [CrossRef]
8. Schwentenwein, M.; Homa, J. Additive manufacturing of dense alumina ceramics. *Int. J. Appl. Ceram. Technol.* **2015**, *12*, 1–7. [CrossRef]
9. Zanchetta, E.; Cattaldo, M.; Franchin, G.; Schwentenwein, M.; Homa, J.; Brusatin, G.; Colombo, P. Stereolithography of SiOC ceramic microcomponents. *Adv. Mater.* **2016**, *28*, 370–376. [CrossRef] [PubMed]
10. Jonušauskas, L.; Baravykas, T.; Andrijec, D.; Gadišauskas, T.; Purlys, V. Stitchless support-free 3D printing of free-form micromechanical structures with feature size on-demand. *Sci. Rep.* **2019**, *9*, 1–12. [CrossRef] [PubMed]
11. Gandy, P.J.; Klinowski, J. Exact computation of the triply periodic Schwarz P minimal surface. *Chem. Phys. Lett.* **2000**, *322*, 579–586. [CrossRef]

12. Fritzsche, S. Available online: https://github.com/BAMresearch/ScaffoldStructures (accessed on 3 March 2022).
13. Dinis, J.C.; Morais, T.F.; Amorim, P.H.J.; Ruben, R.B.; Almeida, H.A.; Inforçati, P.N.; Bártolo, P.J.; Silva, J.V.L. Open source software for the automatic design of scaffold structures for tissue engineering applications. *Procedia Technol.* **2014**, *16*, 1542–1547. [CrossRef]
14. Ultimaker Cura Software. Available online: https://ultimaker.com/de/software/ultimaker-cura (accessed on 1 January 2022).

Disclaimer/Publisher's Note: The statements, opinions and data contained in all publications are solely those of the individual author(s) and contributor(s) and not of MDPI and/or the editor(s). MDPI and/or the editor(s) disclaim responsibility for any injury to people or property resulting from any ideas, methods, instructions or products referred to in the content.